



**HAL**  
open science

## Rising bubble near a free surface: numerical and asymptotic study

Marine Guémas, Franck Pigeonneau, Antoine Sellier

► **To cite this version:**

Marine Guémas, Franck Pigeonneau, Antoine Sellier. Rising bubble near a free surface: numerical and asymptotic study. International Conference on Multiphase Flow, May 2013, Jeju, South Korea. hal-01519290

**HAL Id: hal-01519290**

**<https://minesparis-psl.hal.science/hal-01519290>**

Submitted on 6 May 2017

**HAL** is a multi-disciplinary open access archive for the deposit and dissemination of scientific research documents, whether they are published or not. The documents may come from teaching and research institutions in France or abroad, or from public or private research centers.

L'archive ouverte pluridisciplinaire **HAL**, est destinée au dépôt et à la diffusion de documents scientifiques de niveau recherche, publiés ou non, émanant des établissements d'enseignement et de recherche français ou étrangers, des laboratoires publics ou privés.

# Rising bubble near a free surface : numerical and asymptotic study

M. Guémas\*, F. Pigeonneau\*, A. Sellier†

\* Surface du Verre et Interfaces, UMR 125 CNRS/Saint-Gobain, Aubervilliers, France

† LadHyx. Ecole polytechnique, 91128 Palaiseau Cédex, France,

**Keywords:** Bubble, free surface, surface tension, Stokes flow, asymptotical expansion, film drainage

## Abstract

Phase separation is involved in many chemical processes and is generally limited by the collapse of inclusions at the free surface. For instance, the coalescence of bubbles in highly viscous Newtonian fluids is observed in various fields, such as geophysics or the glass industry.

When a bubble rises through a liquid toward a free surface, we first observe the rising of the bubble driven by the buoyancy forces. In the second step corresponding to the drainage, a liquid film is created between the bubble interface and the free surface decreasing with the time. Both the bubble shape close to the free surface and the film thickness depend upon on the Bond number which is the ratio of gravity to surface tension forces.

Under the assumption of the small Reynolds number, the inertial effects are neglected. Moreover, both the surface tensions of the free surface and the bubble are assumed uniform but their values can be different. We have already investigated the gravity-driven migration using a numerical method based on the boundary-integral method (Pigeonneau and Sellier (2011)). The aim of the current work is to develop an asymptotic solution when the Bond number is small.

In the perturbation method, the interfaces and flow are developed following an asymptotic expansion for which the small parameter is the Bond number. The zeroth order corresponds to the case of undeformed interfaces (flat free surface and spherical bubble) which can be determined using bipolar coordinates. The hydrodynamic force at the zeroth order is obtained using the exact solution provided by Stimson and Jeffery (1926).

The behavior of the film thickness is obtained from the momentum equation on the bubble. We compare the asymptotic predictions with the previous numerical results. Finally, the bubble and free surface shapes are investigated for different values of the surface tension ratio and small Bond number.

## 1. Introduction

The problem of bubble deformation and migration in the presence of a free surface occurs in many multi-phase flows applications, such as phase separation or foam production. The motion of a bubble driven by the gravity in a viscous flow toward a free surface is of particular interest in such varied fields as glass process or biomechanics application. As one bubble approaches a free surface the hydrodynamic interaction affect the shapes of the bubble and of the interface. This problem has been numerically investigated by Pigeonneau and Sellier (2011) who examined the deformations, versus the Bond number (see definition in §2.2), of interacting free surface and bubble(s). This was performed for axisymmetric free surface and bubble having the same axis of revolution parallel with the applied gravity field and the *same* uniform surface tension. This work was recently extended in Guémas et al. (2012) to the

case  $\gamma_0 \neq \gamma_1$ . Nevertheless, numerical troubles occur for small Bond number. Therefore, this work asymptotically obtains the free surface and bubble shapes when  $Bo \ll 1$ . This is achieved here by mimicking the treatment employed in Chervenivanova and Zapryanov (1985) for a droplet.

## 2. Governing problem

### 2.1. Axisymmetric problem

As depicted in Fig. 1, we look at a bubble  $B_1$  driven by buoyancy effects toward a free surface  $S_0$ . The liquid surrounding the bubble is a Newtonian fluid with uniform density  $\rho$  and viscosity  $\mu$ . The bubble is subject to a uniform gravity  $\mathbf{g} = -g\mathbf{e}_z$  with magnitude  $g$  and the ambient fluid above the free surface is a gas with a uniform pressure  $p_0$ . Both the temperature  $T_1$  and the

pressure  $p_1$  inside the bubble are assumed uniform and constant in time. The bubble surface  $S_1(t)$  and the free surface  $S_0(t)$  have uniform surface tension  $\gamma_1 > 0$  and  $\gamma_0 > 0$ , respectively.

As the bubble approaches the free surface, the shape of each surface evolves in time. At initial time, the bubble is taken spherical with radius  $a$  and the free surface is the  $z = 0$  plane. At any time  $t$ , the deformed bubble surface  $S_1(t)$  and free surface  $S_0(t)$  are axisymmetric, having identical axis of revolution parallel with the gravity  $\mathbf{g}$ , and the flow in the liquid domain  $D(t)$  has pressure  $p + \rho\mathbf{g}\cdot\mathbf{x}$  and velocity  $\mathbf{u}$  with typical magnitude  $U$ . All inertial effect are neglected, i.e the Reynolds number  $Re$  obeys  $Re = \rho U a / \mu \ll 1$ .

Assuming quasi-steady bubble and free surface deformations, the flow  $(\mathbf{u}, p)$  then satisfies the following far-field behavior and Stokes equations

$$\begin{aligned} \mu \nabla^2 \mathbf{u} &= \mathbf{grad}[p] \quad \text{and} \quad \nabla \cdot \mathbf{u} = 0 \quad \text{in } D(t), \\ (\mathbf{u}, p) &\rightarrow (\mathbf{0}, 0) \quad \text{as} \quad |\mathbf{x}| \rightarrow \infty \end{aligned} \quad (1)$$

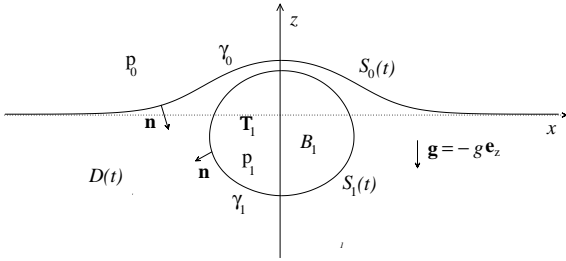


**Figure 1:** One bubble  $B_1$  ascending near a free surface  $S_0(t)$ .

The flow  $(\mathbf{u}, p)$  has stress tensor  $\boldsymbol{\sigma}$  and, denoting (see Fig.1) by  $\mathbf{n}$  the unit normal on  $S_0(t) \cup S_1(t)$  directed into the liquid, one also requires the boundary condition

$$\boldsymbol{\sigma} \cdot \mathbf{n} = (\rho\mathbf{g} \cdot \mathbf{x} - p_m + \gamma_m \nabla_S \cdot \mathbf{n}) \cdot \mathbf{n} \quad \text{on } S_m(t) \text{ for } m = 0, 1 \quad (2)$$

where  $[\nabla_S \cdot \mathbf{n}]/2 = H$  is the local average curvature ( $[\nabla_S \cdot \mathbf{n}]$  is the surface divergence of the unit normal  $\mathbf{n}$ ). Moreover, there is no mass transfer across the liquid boundary which implies that

$$\mathbf{v} \cdot \mathbf{n} = \mathbf{u} \cdot \mathbf{n} \quad \text{on } S_m(t) \text{ for } m = 0, 1 \quad (3)$$

with  $\mathbf{v}$  the material velocity on each surface  $S_m(t)$ . One also requests a time-independent bubble volume. Since  $\mathbf{u}$  is divergence-free, this results in the following

conditions

$$\int_{S_m} \mathbf{u} \cdot \mathbf{n} \, dS = 0 \quad \text{for } m=0,1. \quad (4)$$

Therefore, the constant volume of the bubble is  $V = 4\pi a^3/3$  where  $a$  is the bubble radius at initial time. Finally, since the bubble has no inertia, the net force on the bubble is zero at any time, i.e.

$$\int_{S_1(t)} \boldsymbol{\sigma} \cdot \mathbf{n} \, dS - \rho V \mathbf{g} = \mathbf{0}. \quad (5)$$

Substituting  $V$  by its expression, we obtain

$$\int_{S_1(t)} \boldsymbol{\sigma} \cdot \mathbf{n} \, dS = -\frac{4\pi\rho g a^3}{3} \mathbf{e}_z. \quad (6)$$

Note that (6) holds at any time.

## 2.2. Dimensionless parameters

From the condition (2) on the stress component, we introduce three dimensionless numbers. First, the Bond number  $Bo$ , associated with the bubble, which compares the body force  $(\rho\mathbf{g} \cdot \mathbf{x}) \cdot \mathbf{n}$  to the capillary surface force  $(\gamma_1(\nabla_S \cdot \mathbf{n}) \cdot \mathbf{n})$ . Second, the free surface capillary number  $Ca$  comparing the viscous force  $(\boldsymbol{\sigma} \cdot \mathbf{n})$  to the capillary surface force  $\gamma_0(\nabla_S \cdot \mathbf{n}) \cdot \mathbf{n}$ . Finally,  $\hat{\gamma}$  designates a surface tension ratio. Taking  $a$  as typical length and  $U$  as velocity scale, these numbers read

$$Bo = \frac{\rho g a^2}{\gamma_1}, \quad Ca = \frac{\mu U}{\gamma_0}, \quad \hat{\gamma} = \frac{\gamma_0}{\gamma_1}. \quad (7)$$

For symmetry reasons, the hydrodynamic force  $\mathbf{F}$  exerted on the bubble admits the following form

$$\mathbf{F} = \int_{S_1(t)} \boldsymbol{\sigma} \cdot \mathbf{n} \, dS = -4\pi\mu U a \lambda \mathbf{e}_z \quad (8)$$

with  $\lambda$  the so-called dimensionless drag.

Recalling (6), we arrive at

$$-4\pi\mu U a \lambda \mathbf{e}_z = -\frac{4}{3}\pi\rho g a^3 \mathbf{e}_z. \quad (9)$$

Accordingly,

$$\lambda U \mu = \frac{\rho g a^2}{3}, \quad Bo = 3\lambda \hat{\gamma} Ca. \quad (10)$$

In the case of a rigid bubble translating in an unbounded viscous liquid at the velocity  $U\mathbf{e}_z$  Hadamard (1911) predicts that  $\lambda = 1$ . Therefore, a rigid (spherical) bubble migrates far from the free surface under the uniform gravity  $\mathbf{g} = -g\mathbf{e}_z$  at the velocity  $U_\infty\mathbf{e}_z$  with  $U_\infty = \rho g a^2 / (3\mu)$ .

### 2.3. Available results and pending issue

This problem has been numerically solved by Pigeonneau and Sellier (2011) for uniform surface tensions  $\gamma_0 = \gamma_1$  by implementing a boundary integral formulation. Recently, Guémas et al. (2012) extended this work to deal with the case  $\hat{\gamma} \neq 1$ . These studies cover a large range of Bond number and deal with large deformations of the interfaces. However, as the Bond number tends to zero, numerical calculations experience troubles. Nevertheless, as the Bond number becomes small we expect the bubble and the free surface to be nearly-spherical and nearly-flat, respectively. This suggests to track the bubble and free surface shapes by achieving an asymptotic analysis versus the small Bond number. Such an analysis is presented in this work.

### 3. Asymptotic analysis

Henceforth, we assume that  $\text{Bo} \ll 1$ . As noticed at the end of §3.1, it can be shown that the dimensionless drag  $\lambda$  is of order unity. Assuming  $\hat{\gamma} = O(1)$ , the relation  $\text{Bo} = 3\lambda \hat{\gamma} \text{Ca}$  yields  $\text{Ca} \ll 1$ .

Therefore, the flow  $(\mathbf{u}, p)$  and its stress tensor  $\boldsymbol{\sigma}$  are expanded in terms of the small parameter  $\text{Ca}$  as follows

$$\begin{cases} \mathbf{u} = \mathbf{u}_0 + \text{Ca} \mathbf{u}_1 + \dots, \\ p = p_0 + \text{Ca} p_1 + \dots, \\ \boldsymbol{\sigma} = \boldsymbol{\sigma}_0 + \text{Ca} \boldsymbol{\sigma}_1 + \dots \end{cases} \quad (11)$$

with  $(\mathbf{u}_0, p_0)$  the Stokes flow about a spherical bubble moving toward a flat free surface.

#### 3.1. Zeroth-order solution $(\mathbf{u}_0, p_0)$

We further adopt cartesian coordinates normalized by the radius  $a$ . As illustrated in Fig. 2, the flow  $(\mathbf{u}_0, p_0)$  is the Stokes flow due to a spherical bubble translating at the velocity  $U\mathbf{e}_z$  toward the flat  $z = 0$  free surface. This flow fulfills the boundary conditions  $\mathbf{u}_0 \cdot \mathbf{e}_z = 0$  at  $z = 0$  and  $\mathbf{u}_0 \cdot \mathbf{n} = U\mathbf{e}_z \cdot \mathbf{n}$  on the bubble surface  $S_1$  having unit outward normal  $\mathbf{n}$ .

This problem has been solved by M. Meyyeppan (1981) using bipolar coordinates  $(\zeta, \eta, \phi)$ . Those coordinates (see Happel and Brenner (1983)) are related to cylindrical coordinates  $(x, z, \phi)$  through the relations

$$z = \frac{c \sinh \zeta}{\cosh \zeta - \cos \eta}, \quad r = \frac{c \sin \eta}{\cosh \zeta - \cos \eta}, \quad (12)$$

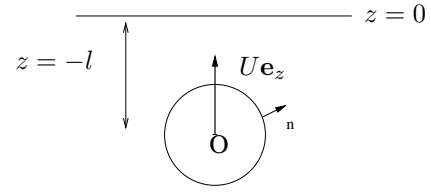


**Figure 2:** One spherical bubble rigidly translating toward the  $z = 0$  flat free surface.

where  $c > 0$ ,  $0 \leq \eta \leq \pi$ ,  $-\infty \leq \zeta \leq \infty$  and  $0 \leq \phi \leq 2\pi$ .

For these coordinates, the surface  $\zeta = \zeta_p > 0$  describes a sphere above the  $z = 0$  plane whereas the surface  $\zeta = -\zeta_p$  describes a sphere below the  $z = 0$  plane. The constant  $\zeta_p$  is moreover related to the lengths as

$$l = \cosh(\zeta_p), \quad c = \sinh(-\zeta_p),$$

where  $l$  is the bubble center distance to the  $z = 0$  plane normalized by  $a$ .

In terms of bipolar coordinates, the boundary conditions satisfied by the zeroth-order flow become

$$\mathbf{u} \cdot \mathbf{n} = 0 \quad \text{at } \zeta = 0 \text{ (free surface)}, \quad (13)$$

$$\mathbf{u} \cdot \mathbf{n} = U\mathbf{e}_z \cdot \mathbf{n} \quad \text{at } \zeta = -\zeta_p \text{ (bubble)}. \quad (14)$$

Since the problem is axisymmetric, it is convenient to introduce a stream function  $U\Psi(\zeta, \chi)$  with  $\chi = \cos(\eta)$ . Then

$$\begin{aligned} u_{0\zeta} &= \mathbf{u}_0 \cdot \mathbf{e}_\zeta = -U \frac{(\cosh(\zeta) - \chi)^2}{c^2} \frac{\partial \Psi}{\partial \chi}, \\ u_{0\eta} &= \mathbf{u}_0 \cdot \mathbf{e}_\eta = -U \frac{(\cosh(\zeta) - \chi)^2}{c^2 \sin(\eta)} \frac{\partial \Psi}{\partial \zeta}, \end{aligned} \quad (15)$$

where  $(\mathbf{e}_\zeta, \mathbf{e}_\eta)$  are the unit vectors for the bipolar coordinates (see Happel and Brenner (1983)).

Appealing to Stimson and Jeffery (1926), one has

$$\Psi(\zeta, \chi) = \frac{1}{(\cosh(\zeta) - \chi)^{\frac{3}{2}}} \sum_{n=1}^{\infty} U_n(\zeta) V_n(\chi) \quad (16)$$

where  $V_n(\chi) = [P_{n-1}(\chi) - P_{n+1}(\chi)]$  with  $P_n(\chi)$  the Legendre polynomial of order  $n$ , and by virtue of the boundary condition (14),

$$U_n(\zeta) = B_n \sinh\left(n - \frac{1}{2}\right)\zeta + D_n \sinh\left(n + \frac{3}{2}\right)\zeta. \quad (17)$$

The coefficients  $B_n$  and  $D_n$  are analytically obtained (and displayed in the Appendix <sup>1</sup>) by enforcing the

<sup>1</sup>These coefficients were given by M. Meyyeppan (1981) but with misprints corrected in the present paper.

boundary condition (13). Once this is done, it is possible to compute the zeroth-order hydrodynamic force  $\mathbf{F}_0$  such that

$$\mathbf{F}_0 = \int_{S_1} \boldsymbol{\sigma}_0 \cdot \mathbf{n} dS = -4\pi\mu U a \lambda_0 \mathbf{e}_z \quad (18)$$

We retrieve that  $\lambda_0 \rightarrow 1$  as  $l \rightarrow \infty$  (Hadamard solution) and also convincing numerical comparisons with Bart (1968) at finite values of  $l$ . These computations show, as previously-announced, that  $\lambda_0 = O(1)$ . Finally, invoking (10) we get  $U = U_\infty/\lambda_0$  with  $U_\infty = \rho g a^2/(3\mu)$ .

### 3.2. First-order, disturbed free-surface and bubble shape

For  $Ca = 0$ , the free surface and the bubble shapes are flat and spherical with equations  $\zeta = 0$  and  $\zeta = -\zeta_p$ , respectively. In the case of  $0 < Ca \ll 1$ , the weakly disturbed shapes admit then the equations

$$\zeta \simeq Ca \zeta_1(\chi), \quad (\text{free surface}) \quad (19)$$

$$\zeta \simeq -\zeta_p + \frac{\gamma_1}{\gamma_0} Ca \zeta_1^b(\chi), \quad (\text{bubble}) \quad (20)$$

with  $\zeta_1$  and  $\zeta_1^b$  two unknown shape functions and  $\chi = \cos \eta \in [-1, 1]$ .

Those functions obeys differential equations established in Chervenivanova and Zapryanov (1985). For the free surface, one obtains

$$\begin{aligned} -2\zeta_1 + (1-\chi)^3 \frac{\partial}{\partial \chi} \left[ \frac{1+\chi}{1-\chi^2} \frac{\partial \zeta_1}{\partial \chi} \right] \\ + \frac{c \text{Bo} \zeta_1}{1-\chi} = \frac{ca}{\mu U} [\mathbf{e}_\zeta \cdot \boldsymbol{\sigma}_0 \cdot \mathbf{e}_\zeta](0, \eta). \end{aligned} \quad (21)$$

Since at infinity (as  $r \rightarrow \infty$ ), the free surface is not disturbed, one requires that

$$\lim_{\chi \rightarrow 1} \frac{\zeta_1}{(1-\chi)} = 0. \quad (22)$$

Chervenivanova and Zapryanov (1985) solved (21)-(22) and predicted a disturbed free surface having a non-horizonthal tangent at  $r = 0$  (i.e. on the  $(0, \mathbf{e}_z)$  axis). However, on theoretical grounds, the smooth disturbed free surface necessarily exhibits a zero slope on the  $(0, \mathbf{e}_z)$  axis of revolution.<sup>2</sup> Therefore, in this work, we supplement (21)-(22) with the additionnal requirement of a zero slope at  $r = 0$  ( $\chi = -1$ ). This condition reads

$$2 \frac{\partial \zeta_1}{\partial \chi} + \zeta_1 = 0. \quad (23)$$

<sup>2</sup>The numerical predictions obtained in Pigeonneau and Sellier (2011) actually comply with this property.

In a similar fashion, the governing equation for the shape function  $\zeta_1^b$  is found in Chervenivanova and Zapryanov (1985) to be

$$\begin{aligned} (\cosh \zeta_p - \chi)^3 \left[ \frac{\partial}{\partial \chi} \frac{1-\chi^2}{(\cosh \zeta_p - \chi)^2} \frac{\partial \zeta_1^b}{\partial \chi} \right] \\ + 2 \zeta_1^b \cosh(\zeta_p) = S, \end{aligned} \quad (24)$$

with the right-hand side  $S$  defined as

$$\begin{aligned} S = - \left[ \frac{ca}{\mu U} [\mathbf{e}_\zeta \cdot \boldsymbol{\sigma}_0 \cdot \mathbf{e}_\zeta] (-\zeta_p, \eta) \right. \\ \left. + 3 \lambda_0 c^2 (\cosh \zeta_p - \chi)^{\frac{1}{2}} \sqrt{2} \right. \\ \left. \sum_{n=1}^{\infty} (2n+1) e^{(n+1)\zeta_p} P_n(\chi) \right]. \end{aligned} \quad (25)$$

Finally, we impose the conservation of the bubble volume and that  $O$  is the bubble center of volume. Those conditions give

$$\int_{-1}^1 \frac{\zeta_1(\chi)}{(\cosh \zeta_p - \chi)^3} d\chi = 0, \quad (26)$$

$$\int_{-1}^1 \frac{\zeta_1(\chi)}{(\cosh \zeta_p - \chi)^4} d\chi = 0 \quad (27)$$

In summary, one has to solve the problem (21)-(23) and (24),(26)-(27).

## 4. Numerical method and preliminary results

### 4.1. Numerical implementation

In this section, we briefly introduce our numerical method to determine the time-dependent free surface and bubble shapes. This is achieved by appealing to the following key steps :

1) Initial data: we prescribe the small Bond number  $\text{Bo} = \rho g a^2/\gamma_1 \ll 1$  and the surface tension ratio  $\hat{\gamma} = \gamma_0/\gamma_1$ . We also give at initial time  $t = 0$  the bubble shape (spherical with given radius  $a$ ) and location below a sufficiently distant flat free surface.

2) At time  $t > 0$ , we know the location of the bubble center of volume  $O$  (i.e. the value of  $l$  as shown in Fig. 2) from the solution at previous times.

2.1) First, we obtain  $\mathbf{u}_0$ ,  $\boldsymbol{\sigma}_0$ ,  $\lambda_0$  and  $U = U_\infty/\lambda_0$  using the solution given in §3.1. We then calculate the associated Capillary number  $Ca = \mu U/\gamma_0 = \text{Bo}/(3\lambda_0 \hat{\gamma})$ .

2.2) Then, we determine the disturbed shapes  $S_0(t)$  and  $S_1(t)$  by solving the problems (21)-(23) and (24),(26)-(27), respectively. By contrast to Chervenivanova and Zapryanov (1985) who employed a decomposition of functions  $\zeta_1$  and  $\zeta_1^b$  in terms of Legendre polynomials, we here directly solve the problem by using a second-order finite difference method scheme (the resulting linear system being solved by a LU factorization).

3) Finally, between time  $t$  and  $t + dt$ , we move the bubble center of volume  $O$  at the velocity  $U \mathbf{e}_z$ .

## 4.2. Results

Some preliminaries results are exposed here.

We compare in Fig. 3 the free surface shapes predicted by the numerical code and the present asymptotic analysis for  $Bo = 0.09$ ,  $\hat{\gamma} = 1$  and  $l = 3.515$ . For this case, one obtains  $Ca \simeq 0.0257$ .

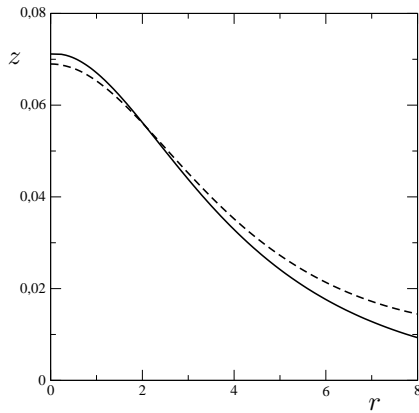


**Figure 3:** Compared free surface profiles. Numerical results (dashed line) and asymptotic analysis (solid line).

As expected, for  $z \gtrsim O(Ca)$  the differences between the two profiles is order  $O(Ca^2)$ .

## 5. Conclusion

For  $Bo \ll 1$ , the weakly disturbed shapes of the free surface and bubbles have been asymptotically obtained at the leading order. Additional comparisons against the direct numerical treatment proposed in Pigeonneau and Sellier (2011) and Guémas et al. (2012) will be addressed at the talk.

## A. Expression of the coefficients $B_n$ and $D_n$

Enforcing the boundary condition (14) and taking into account of (15)-(16), one gets

$$B_n = \frac{k_n [e^{-2\zeta_p} - e^{(2n+1)\zeta_p}]}{(2n-1)[\cosh(2n+1)\zeta_p - \cosh 2\zeta_p]} \quad (28)$$

$$D_n = \frac{k_n [e^{(2n+1)\zeta_p} - e^{2\zeta_p}]}{(2n+3)[\cosh(2n+1)\zeta_p - \cosh 2\zeta_p]} \quad (29)$$

where  $k_n = \frac{c^2 n(2n+1)}{\sqrt{2}(2n+1)}$ .

## References

- E. Bart. The slow unsteady settling of a fluid sphere toward a flat fluid interface. *Chem. Eng. Sci.*, 23:193–210, 1968.
- E. Chervenivanova and Z. Zapryanov. On the deformation of two droplets in a quasisteady Stokes flow. *int. J. Multiphase Flow*, 11:721–738, 1985.
- M. Guémas, F. Pigeonneau, and A. Sellier. Gravity-driven migration of one bubble near a free surface: surface tension effects. In M. H. Aliabadi P. Prochazca, editor, *Advances in Boundary Element & Meshless Techniques XIII*, 2012.
- J. Hadamard. Mouvement permanent lent d’une sphère liquide et visqueuse dans un liquide visqueux. *C. R. Acad. Sci. Paris*, 152:1735–1738, 1911.
- J. Happel and H. Brenner. *Low Reynolds number hydrodynamics*. Martinus Nijhoff Publishers, The Hague, 1983.
- R. Shankar Subramanian M. Meyyeppan, W. R. Wilcox. Thermocapillary migration of a bubble normal to a plane surface. *Journal of Colloid and Interface Science*, 83: 199–208, 1981.
- F. Pigeonneau and A. Sellier. Low-reynolds-number gravity-driven migration and deformation of bubbles near a free surface. *Phys. Fluids*, 23:092302, 2011.
- M. Stimson and G. B. Jeffery. The motion of two spheres in a viscous fluid. *Prod. R. Soc. London, Serie A*, 111: 110–116, 1926.